Available online at www.sciencedirect.com
ScienceDirect
Engineering Structures 30 (2008) 450–461
ENGINEERING STRUCTURES
www.elsevier.com/locate/engstruct

Detailing procedures for seismic rehabilitation of reinforced concrete members with fiber reinforced polymers

S.P. Tastani*, S.J. Pantazopoulou

Demokritus University of Thrace (DUTh), Vas. Sofias Street No. 1, Xanthi 67100, Greece

Received 9 August 2005; received in revised form 31 January 2007; accepted 22 March 2007
Available online 25 May 2007

Abstract

Fiber reinforced polymer jackets (FRP sheets) offer great advantages as confining devices of damaged or substandard reinforced concrete (r.c.) members and are already used extensively as local interventions in seismic rehabilitation of existing construction. The design issues and detailing rules related to this seismic repair/strengthening technique are explored by evaluating systematically the various mechanisms of resistance of the upgraded member and the jacket contribution. These include flexure, shear, lap-splice capacity, plastic hinge behavior, displacement capacity and jacket strain capacity associated with embedded bar buckling. A database of published experiments on r.c. beam/columns, tested under cyclic loading after being jacketed by FRPs was used as a point of reference in assessing the detailing rules and in calibrating design lower bound expressions. Criteria that should be considered for the upgrade design strategy in order to control the deformation demand of the structure when FRP jackets are used are also discussed in the paper.

Keywords: FRP jacketing; Repair; Strengthening; Seismic upgrading; Design

1. Introduction

A basic ailment of many of the r.c. structures that get damaged during earthquakes is intrinsic lack of stiffness (e.g. in soft storey formations), combined with limited deformation capacity of the individual structural elements owing to non-ductile, old type detailing. Because excessive displacement brings out all the potential problems of an inadequate design or construction, it is necessary in repair/strengthening schemes to target for reduced displacement demand, by increasing the lateral stiffness of the structure. The necessary global interventions are accompanied by targeted local measures aiming to increase the dependable deformation capacity of the individual members so that the supply exceeds the deformation demand.

Rehabilitation of damaged or under-designed r.c. beam and columns with FRP jacketing belongs to the class of local interventions. In the context of this paper, the expression *FRP jacketing* refers to any type of application of the material where the primary fibers are oriented transversally to the longitudinal axis of the upgraded member and at a minimum of three faces of the member's cross section so as to facilitate confining action against any dilation of the concrete (i.e. due to axial load, shear transverse tension or dilation produced by the bond action of a ribbed bar). Although FRP jackets are effective in upgrading shear strength, lap splice strength, and overall flexural and shear deformation capacity, they combine three characteristics that may prevail and control failure in a flexible structure. Thus, (a) they have negligible influence on the lateral stiffness of the jacketed member. Unless the transverse jackets serve to mitigate premature local failures that would otherwise limit the pre-yield response, secant to yield stiffness (EI) remains unaltered by the repair. (b) They are susceptible to rupture at points of localized deformation demand. Although they can substantially increase the compression strain capacity of encased concrete, they delay but cannot preclude eventual buckling of compression reinforcement and the ensuing collapse of the member. (c) They effectively reduce shear cracking in the plastic hinge regions, driving all deformation to occur within a few flexural cracks

* Corresponding author. Tel.: +30 25410 79639; fax: +30 25410 79639.
E-mail addresses: stastani@civil.duth.gr (S.P. Tastani), pantaz@civil.duth.gr (S.J. Pantazopoulou).

0141-0296/$ - see front matter © 2007 Elsevier Ltd. All rights reserved.
doi:10.1016/j.engstruct.2007.03.028

Nomenclature

A_{st} cross-sectional area of stirrup legs in a single stirrup layer (mm^2).
A_g cross-sectional area of r.c. member (mm^2).
b cross-sectional width (mm).
c clear cover of steel reinforcement (mm).
d cross-sectional effective depth (mm).
D_b longitudinal bar diameter (mm).
E_f modulus of elasticity of the FRP (GPa).
f_b average bond stress (MPa).
f'_c, f'_t uniaxial compressive and tensile strength of concrete (MPa).
f'_{cc} confined compressive strength of concrete (MPa).
f_{fb}, $f_{fb,d}$ average bond stress and design value of the FRP sheet (MPa).
f_{fu} nominal rupture stress of FRP material (MPa).
$f_{gl,d}$ design shear strength of the resin (MPa).
$f_{s,\text{crit}}$ critical buckling stress of compression reinforcement (MPa).
f_y,$f_{y,\text{st}}$ yield stress of longitudinal and transverse reinforcement (MPa).
h cross-sectional height (mm).
k_f, k_{st} effectiveness coefficients of FRP jacket and stirrups. Superscript v refers to the shear effectiveness, *anch* to the anchorage effectiveness and c to confinement effectiveness.
L_b, L_f development length of longitudinal bar and FRP ply, respectively (mm).
l_p plastic hinge length (mm).
L_s shear span of the r.c. member (mm).
n number of FRP layers.
N_b number of longitudinal bars.
P axial load on the cross section (in N).
q or R behavior factor.
s spacing of stirrups (mm).
$s_{gl,u}$ slip of the resin (mm).
t_f FRP ply thickness (mm).
w_{cr} crack width (mm).
Δ_y, Δ_u yielding and ultimate displacement (mm).
$\varepsilon_{c,u}$, $\varepsilon_{cc,u}$ failure strain of unconfined and confined concrete.
ε_{co}, ε_{cc} uniaxial compressive strain at f'_c and at f'_{cc}.
ε_f^{eff} effective tensile strain of the FRP jacket.
$\varepsilon_{fu,d}$ nominal deformation capacity of the FRP material.
$\varepsilon_{s,\text{crit}}$ critical buckling strain of compression reinforcement.
$\varepsilon_{s,cu}$ strain of the compression reinforcement corresponding to $\varepsilon_{cc,u}$.
ε_y yield strain of longitudinal reinforcement.
ϕ_y/ϕ_u yielding and ultimate curvature (1/mm)
γ_{fb} material safety factor for the relationship between characteristic and design bond strength
μ coefficient of friction at the steel–concrete interface.
$\mu_\Delta, \mu_\phi, \mu_\varepsilon$ displacement, curvature and compression strain ductility.
ρ_{fv}, ρ_{sv} volumetric ratio of FRP jacket and stirrups.
ρ_{fy}, ρ_{sy} transverse FRP and steel ratio.
σ_{lat} passive pressure; superscripts f and st refer to pressures applied by FRP and stirrups (MPa).

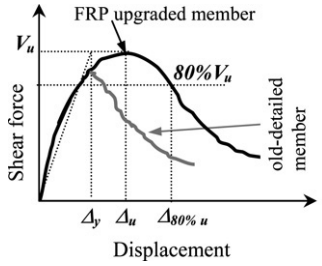

Fig. 1. Improvement of response due to FRP jacketing—definition of deformation indices.

near the face of the support. Confinement enables attainment of high strain demands in the tension reinforcement at the critical section. The increased demand for bar development capacity cannot always be met by the anchorage which is often inadequate in substandard construction and inaccessible to rehabilitation (Tastani and Pantazopoulou [1]).

As a local intervention, FRP jacketing needs be explicitly embedded in the context of the integrated global strategy of seismic rehabilitation of the structure, where, survivability of the upgraded structural system depends on the magnitude of the lateral drift. In the paper, the first sections consider the confining pressure generated by the FRP, its effectiveness, and the design effective strain that may be used in calculations. The derived expressions are used next to obtain the various strength terms and the deformation capacity of FRP jacketed r.c. members. Considerations about drift control that need be combined with the FRP jacketing are discussed and the entire procedure is applied in a building case study using the Yield Point Spectrum Method to guide the upgrading strategy.

2. Mechanical effects of FRP jacketing on r.c. members

In selecting FRP jacketing for seismic upgrading, the repair objective is restricted to maintaining or marginally increasing the flexural strength of the members without influencing their initial stiffness (Fig. 1), up to full exploitation of the deformation capacity of longitudinal reinforcement. The actual increase in strength and deformation capacity effected through FRP jacketing may be quantified by approaches similar to those used in the case of conventionally r.c. members. ACI 440.2R-02 [2] presents expressions for calculation of strength enhancement and design recommendations.

As with stirrups, the jacket is mobilized in tension when the encased concrete dilates laterally. Lateral expansion (resembling Poisson's effect in elastic media) occurs in concrete when the material is under significant axial compressive stress. The FRP jacket acts as passive confinement

by restraining dilation, thereby enhancing the deformation capacity of confined concrete (Pantazopoulou [3]). In r.c. members with sparse stirrups the poorly supported longitudinal compression reinforcement tends to buckle outwards at large compression strains. In these cases the FRP jacket resists stress concentrations along the buckling rebars. Web dilation also occurs in the presence of significant shear action (web cracking due to diagonal tension failure of concrete). In this case the FRP jacket functions as the tension tie in a strut-and-tie analog of the shear resisting mechanism of the concrete member. FRP wrapping over the embedment length of bar anchorages provides clamping, resisting propagation of cover splitting thereby enhancing the frictional mechanism of bond resistance.

Depending on the function of the jacket in the rehabilitation scheme, either the transverse pressure in the x or y direction ($\sigma_{\text{lat},x}$, $\sigma_{\text{lat},y}$), or the average pressure in two orthogonal directions $\sigma_{\text{lat}}^{\text{ave}} = 0.5(\sigma_{\text{lat},x} + \sigma_{\text{lat},y})$ may be needed to quantify the mechanical function of pressure on resistance. In any given direction of action y, the total transverse pressure, $\sigma_{\text{lat},y}$, comprises contributions of the FRP jacket and the occasional embedded stirrups:

$$\sigma_{\text{lat},y} = \sigma_{\text{lat},y}^{f} + \sigma_{\text{lat},y}^{st} = 2\frac{k_{f,y} n t_f E_f \varepsilon_f^{\text{eff}}}{b} + \frac{k_{st,y} A_{\text{st}} f_{y,\text{st}}}{sb}. \quad (1)$$

Parameters $k_{f,y}$ and $k_{st,y}$ are the effectiveness coefficients for the two transverse confining systems in the direction of interest y (i.e. intersecting the plane of failure), $\varepsilon_f^{\text{eff}}$ is the effective tensile strain that develops in the jacket near failure (which may occur either by debonding or by rupture, whichever prevails), E_f, n, t_f are the elastic modulus, the number of plies and the thickness of an FRP ply, b is the cross-section width at the splitting plane (orthogonal to the applied jacket force), A_{st} is the total cross-sectional area of stirrup legs crossing the splitting plane provided by a single stirrup layer, s the longitudinal spacing of stirrups and $f_{y,\text{st}}$ their yield stress.

2.1. Effectiveness coefficients for the various response mechanisms

The effectiveness coefficients $k_{f,y}$ and $k_{st,y}$ in (1) for the two transverse reinforcement systems *depend upon the function* of $\sigma_{\text{lat},y}$ in the response mechanism considered:

For *shear strengthening*, $k_{f,y}$ depends on the development capacity of the jacket anchorage, whereas $k_{st,y} = 1$ for well anchored closed stirrups. Consider a shear crack extending at 45° along the web height d_f (Fig. 2(a)); transverse pressure develops in the y direction (along the web height). The wrapped jacket is called on to develop its design strain at the critical section, which is at the point of intersection with the crack. If the jacket is closed (i.e., four-sided, well anchored application), then $k_{f,y} = 1$ (Fig. 2(b)). If, owing to the cross-sectional shape of the member it is not possible to wrap the jacket around the section, thus terminating it on the web near the compression zone, (e.g. near the underside of the flange in T-beams, Fig. 2(a)), then, only those fibers that have sufficient anchorage length L_f beyond the crack may be considered

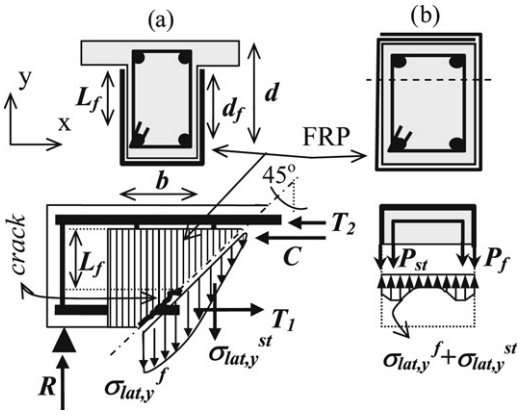

Fig. 2. (a) Free body diagram of FRP wrapped member at a shear crack plane and (b) stress state of FRP strengthened rectangular cross section.

effective as shear reinforcement (here the presence of possible mechanical anchorage means is not considered). In this case, the effectiveness coefficient is $k_{f,y} = (d_f - L_f)/d_f < 1$; in direct analogy, for open shear links, $k_{st,y} = 0.5$ (FIB Bulletin 24 [4]). ACI 440.2R-02 [2] proposes methods for calculating L_f (this is also discussed in the following sections).

When strengthening *for confinement*, the confining pressure is the average value $\sigma_{\text{lat}}^{\text{ave}}$ obtained from (1) in the two principal directions of the cross section as $\sigma_{\text{lat-}x}$ and $\sigma_{\text{lat-}y}$:

$$\sigma_{\text{lat}}^{\text{ave}} = 0.5\left(\sigma_{\text{lat},y} + \sigma_{\text{lat},x}\right) = 0.5\left(k_f^c \rho_{fv} E_f \varepsilon_f^{\text{eff}} + k_{\text{st}}^c \rho_{sv} f_{y,\text{st}}\right) \quad (2)$$

where, $\rho_{fv} = 2nt_f(b+h)/(bh)$ and $\rho_{sv} = (b+h)A_{\text{st}}/(bhs)$ are the volumetric ratios of FRP and stirrup reinforcement (h is the cross-section height). The expression for calculating k_f^c approximates the volume fraction of core concrete that is effectively restrained (similar to the approach used to evaluate confinement effectiveness of stirrups k_{st}^c (Priestley et al. [5]). Therefore, $k_f^c = 1 - (b'^2 + d'^2)/[3A_g(1-\rho_s)]$, where A_g is the gross cross section of the element, ρ_s is the ratio of longitudinal reinforcement, and b' and d' the straight sides of the rectangular cross section encased by the jacket after chamfering the corners (ACI 440.2R-02 [2], FIB Bulletin 14 [6]). Thus, for a cross section with a side aspect ratio of 3, the confinement effectiveness coefficient becomes negligible ($k_f^c \approx 0$), whereas for square and circular cross sections $k_f^c \approx 0.5$ and 1, respectively. Therefore, the primary function of FRP wrapping in a cross section with a very large aspect ratio would be to increase its *lateral load* resistance rather than its axial load strength (i.e., in these cases any reference to strength increase owing to confinement may be neglected).

When strengthening bar *anchorages or lap splices* through transverse restraint the effectiveness coefficients $k_{f,y}^{\text{anch}}$, $k_{st,y}^{\text{anch}}$ take into account how uniform is the restraint provided though the FRP jacket or the stirrups: for the continuous FRP jacket $k_{f,y}^{\text{anch}} = 1$ whereas $k_{st,y}^{\text{anch}} \approx 0.33$ for stirrups to account for their spacing (i.e. reduced efficiency) along the anchorage length as per ACI 318-02 [7], Fig. 3. The splitting plane may occur either starting from an anchored bar and extending towards the nearest free surface, or may cross several bars. Depending

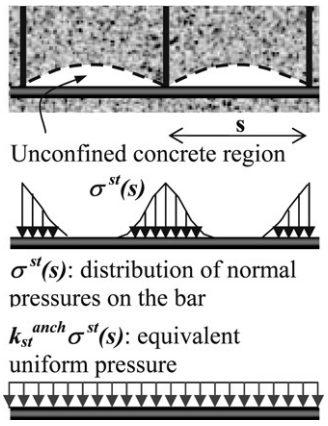

Fig. 3. Definition of the effectiveness coefficient of stirrups $k_{\mathrm{st}}^{\mathrm{anch}}$ for anchorage restraint: $k_{\mathrm{st}}^{\mathrm{anch}}$ averages stirrup stress along their spacing s.

on the direction of splitting, the restraining pressure (and the associated terms in (1)) may be in either of the two principal directions of the cross section.

2.1.1. Derivation of the effective strain, $\varepsilon_f^{\mathrm{eff}}$

The effective strain $\varepsilon_f^{\mathrm{eff}}$ in (1) and (2) is the usable tensile strain capacity of the FRP jacket. In general, $\varepsilon_f^{\mathrm{eff}}$ is only a fraction of the nominal deformation capacity of the material ($\varepsilon_{fu,d}$). The value of $\varepsilon_f^{\mathrm{eff}}$ depends on the mode of failure of the bonded layer that in turn is controlled by the bond strength of the substrate. Choosing a reliable value for $\varepsilon_f^{\mathrm{eff}}$ is a critical step in establishing the contribution of jacket stresses to any failure mechanism of concrete. In the following, $\varepsilon_f^{\mathrm{eff}}$ is defined depending on the jacket geometry (open or closed) and the likely mode of failure of the wrap.

In *open* jackets (i.e., wrapping layers that cannot be fully closed around the cross section) the bonding substrate is the concrete cover and failure may occur by either debonding of the FRP jacket or by *diagonal tension failure* of the cover layer (Fig. 4). Debonding refers to detachment of the wrap from its ends, drawing away a thin layer of concrete along with the bonding interface (Brẽna et al. [8], Fig. 4(a)). Failure of the FRP jacket is controlled by the low resistance of the cover concrete to direct tension. If debonding is suppressed by mechanical anchorage in the ends, the likely mode of failure is diagonal cracking of the cover near pre-existing cracks. Note that the FRP sheet develops forces in tension when crossing cracks in concrete by shearing the substrate. Rather than slipping relative to its surroundings, the composite jacket drags the concrete cover in shear distortion so as to bridge the crack width, leading to premature diagonal tension failure of the concrete cover prior to realization of the jacket's tensile strength. Therefore, this mode of failure is controlled by the width w_{cr}, of the cracks developing in the strengthened member under the wrap (Fig. 4(b)). Assuming a linear variation of jacket stresses over the development length L_f (Fig. 2(a)), the strain $\varepsilon_f^{\mathrm{eff}}$ of the FRP layer at the crack is related to w_{cr} as follows:

$$\frac{w_{\mathrm{cr}}}{2} = \frac{1}{2}\varepsilon_f^{\mathrm{eff}} L_f. \tag{3}$$

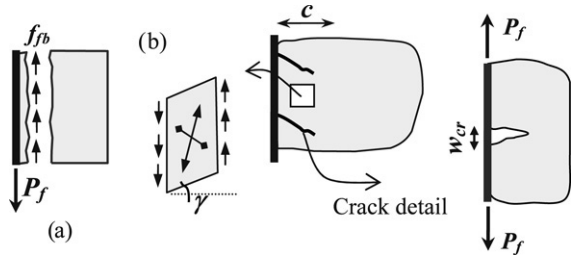

Fig. 4. Failure of *open* jacket by (a) delaminating from concrete and (b) diagonal tension of the cover.

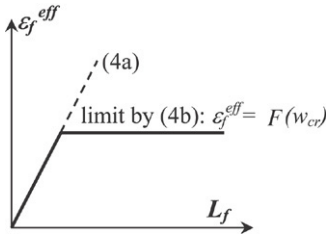

Fig. 5. Strain vs. development length of the FRP layer.

Force equilibrium over the development length requires:

$$\begin{aligned} \varepsilon_f^{\mathrm{eff}} E_f n t_f &= \int_0^{L_f} f_{fb}\,\mathrm{d}x = \frac{f_{fb,k}}{\gamma_{fb}} L_f \\ \Rightarrow \varepsilon_f^{\mathrm{eff}} &= \frac{f_{fb,k} L_f}{\gamma_{fb} E_f n t_f} = \frac{f_{fb,d} L_f}{E_f n t_f}; \\ \text{where } f_{fb,d} &= \frac{f_{fb,k}}{\gamma_{fb}} \end{aligned} \tag{4a}$$

where f_{fb} is the bond stress distribution over the length L_f, $f_{fb,k}$ and $f_{fb,d}$ the characteristic and average design values and γ_{fb} the material safety factor. $f_{fb,k}$ is taken here equal to the tensile strength of the concrete, f_t' and γ_b is taken equal to 2. The strain $\varepsilon_f^{\mathrm{eff}}$ that may develop at the critical section is linearly related to the available development length, L_f (Fig. 4(a)). Substituting (3) in (4a) it may be shown that

$$\varepsilon_f^{\mathrm{eff}} = \sqrt{\frac{w_{\mathrm{cr}} f_{fb,d}}{E_f n t_f}}; \qquad L_f = \sqrt{\frac{w_{\mathrm{cr}} E_f n t_f}{f_{fb,d}}}. \tag{4b}$$

Considering that shear distortion $\gamma = 0.5 w_{\mathrm{cr}}/c$, where c is the cover thickness, becomes prohibitively large for crack widths in excess of 0.3 mm, the results of (4b) are capped by this limiting value for w_{cr} (Fig. 5). Thus, the larger the axial stiffness of the FRP sheet, the lower the strain that may be developed over the sheet anchorage, whereas the usable fraction of its strain capacity is limited by cracking of the substrate. For usual values of the design parameters ($t_f = 0.13$ mm, $E_f = 200$ GPa, $f_{fb,k} = f_t' = 2$ MPa) it follows from (4b) that $\varepsilon_f^{\mathrm{eff}} = 0.0034$, $L_f = 88$ mm.

In *closed jackets*: $\varepsilon_f^{\mathrm{eff}}$ is calculated in a similar manner. Here the weak link is the adhesive resin, stressed in shear along the overlap length, L_f, of each layer. Most critical is the external layer, since the shear strength of the adhesive in interior layers

is enhanced by friction due to confinement. The strength of the bonded system is controlled by the limiting slip $s_{gl,u}$ of the adhesive at shear failure:

$$\left.\begin{array}{l} s_{u,gl} = \varepsilon_f^{\text{eff}} L_f \\ \varepsilon_f^{\text{eff}} E_f t_f = f_{gl,d} L_f \end{array}\right\} \Rightarrow \varepsilon_f^{\text{eff}} = \sqrt{\frac{f_{gl,d} s_{u,gl}}{E_f t_f}};$$

$$L_f = \sqrt{\frac{s_{u,gl} E_f t_f}{f_{gl,d}}} \tag{4c}$$

where $f_{gl,d}$ is the shear strength of the adhesive at the stage of plastification. For illustrative purposes consider the following example: $f_{gl,d} = 5$ MPa, $s_{u,gl} = 1$ mm, $E_f = 200$ GPa, and $t_f = 0.13$ mm, barring any stress concentrations that would accelerate jacket failure, it follows that $\varepsilon_f^{\text{eff}} = 0.0138$, and $L_f = 72$ mm. Clearly the input data to this calculation depend on the adhesive properties; a very large range of products is available and used in FRP applications. Thus, a detailed study of FRP lap-splice development capacities would be needed before design values may be proposed for practical applications.

According to ACI 440.2R-02 [2] the allowable values for $\varepsilon_f^{\text{eff}}$ under monotonic loads are 0.004 and $0.75\varepsilon_{fu,d}$ for open and closed jackets, respectively. Results from compression tests with closed FRP jackets (Chaallal et al. [9]) indicate that the material factor of 0.75 is rather high when used with rectangular cross sections due to the jacket's susceptibility to local rupture at the corners even after chamfering. A value of 0.5 has been found more conservative in this case (i.e., $\varepsilon_f^{\text{eff}} = 0.5\varepsilon_{fu,d}$, Tastani and Pantazopoulou [1]).

3. Strength assessment of FRP rehabilitated r.c. members

In redesigning a substandard r.c. element for seismic resistance the objective is to mitigate all failure modes except flexural, which is the most desirable. Design forces must satisfy the following qualitative relationship:

$$V_{u,\text{lim}} = \min\{V_{\text{iflex}}, V_{\text{shear}}, V_{\text{anch}}, V_{\text{buckl}}\} \tag{5}$$

where, $V_{\text{iflex}} = M_u/L_s$ is the seismic shear force required to develop the ideal flexural resistance of the member, L_s is the shear span, V_{shear} is the nominal shear resistance, V_{anch} is the member shear force when the anchorage/lap-splice reach their development capacity and V_{buckl} is the member shear force when compression reinforcement reaches buckling conditions at the critical section. The strength components in (5) may be estimated from variables $\sigma_{\text{lat},x}$, $\sigma_{\text{lat},y}$ and $\sigma_{\text{lat}}^{\text{ave}}$, calculated by (1) and (2). The necessary calculation steps are presented below.

3.1. Ideal flexural capacity calculations

Flexural resistance is influenced by the concrete strength increase owing to confinement, and the containment of the cover region that would otherwise have spalled-off at ultimate. The confined concrete strength f'_{cc} and the corresponding strain at attainment of peak stress, ε_{cc}, in the compression zone of the encased cross section is calculated from the classical confinement model of Richart et al. [10]:

$$f'_{cc} = f'_c + 4.1\sigma_{\text{lat}}^{\text{ave}}; \qquad \varepsilon_{cc} = \varepsilon_{co}\left(1 + 5\left(\frac{f'_{cc}}{f'_c} - 1\right)\right). \tag{6}$$

Experimental results from FRP-confined concrete cylinders point to a reduced effect of transverse pressure on confined compressive strength (Tastani et al. [11], a multiplier of 3 rather than 4.1 operating on $\sigma_{\text{lat}}^{\text{ave}}$). By substitution of (2) in (6), and assuming $\varepsilon_{co} = 0.002$ (strain at peak stress of unconfined concrete), the following are obtained:

$$f'_{cc} = f'_c + 1.5\left(k_f^c \rho_{fv} E_f \varepsilon_f^{\text{eff}} + k_{\text{st}}^c \rho_{sv} f_{y,\text{st}}\right)$$

$$\varepsilon_{cc} = 0.002 + 0.015\frac{k_f^c \rho_{fv} E_f \varepsilon_f^{\text{eff}} + k_{\text{st}}^c \rho_{sv} f_{y,\text{st}}}{f'_c}. \tag{7}$$

The failure strain $\varepsilon_{cc,u}$ corresponding to a compression strength reduction in excess of 15% is obtained from two alternative expressions:

(a) Priestley et al. [5] have proposed:

$$\varepsilon_{cc,u} = 0.004 + 1.25\frac{k_f^c \rho_{fv} E_f (\varepsilon_f^{\text{eff}})^2}{f'_{cc}}. \tag{8a}$$

(b) A lower bound expression has been calibrated with test results (Pantazopoulou [3]):

$$\varepsilon_{cc,u} = \varepsilon_{c,u} + 0.075 \times \left(\frac{k_f^c \rho_{fv} E_f \varepsilon_f^{\text{eff}} + k_{\text{st}}^c \rho_{sv} f_{y,\text{st}}}{f'_c} - 0.1\right) \geqslant \varepsilon_{c,u};$$

$$0.003 \leqslant \varepsilon_{c,u} \leqslant 0.004. \tag{8b}$$

For closed jackets, $\varepsilon_f^{\text{eff}} = 0.5\varepsilon_{fu,d}$. Note that being a lower bound, (8b) is rather conservative.

3.2. Shear strength calculations

Shear resistance of r.c. members subjected to displacement reversals degrades with the number of cycles and the magnitude of imposed displacement ductility, owing to breakdown of concrete's tensile and compressive resistance with increasing crack widths. This strength reduction is accounted for using a ductility dependent softening coefficient λ (Moehle et al. [12]) as:

$$V_n(\mu_\Delta) = \lambda\,(V_s + V_c);\ \lambda = 1.15 - 0.075\mu_\Delta;\ 0.7 \leqslant \lambda \leqslant 1$$

$$V_s = \sigma_{\text{lat}}^{st} bd$$

$$\text{Moehle et al. [12]}:\ V_c = \frac{6\sqrt{f'_c}}{a/d}\sqrt{1 + \frac{P}{6\sqrt{f'_c}\cdot A_g}}\cdot A_g \quad (f'_c \text{ in psi})$$

$$\text{EKOS-2000}:\ V_c = \beta\cdot\left[\tau_{Rd} k\,(1.2 + 40\rho_l) + 0.15\frac{P}{A_g}\right]\cdot bd(N). \tag{9}$$

In the expression for V_c given by Moehle et al. [12] P is the axial load on the section, α is the distance from

maximum moment to inflection point. In the Greek Design Code (EKOS-2000, [13]) parameter β takes into account the type of r.c. member (plate/shell or linear) in combination with the magnitude of axial load (i.e. $\beta = 0.3$ for seismic design of column and beam where the axial load is $P \leqslant 0.1bhf'_c$, 0.9 for higher axial loads), τ_{Rd} is the shear strength of plain concrete ($=0.25f'_t$), k is a size-effect factor ($=1.6 - d \geqslant 1$, d in m) and ρ_l is the ratio of longitudinal reinforcement that acts as dowels. Factor μ_Δ is the imposed displacement ductility. Parameter A_g is the cross section area of the r.c. member. The transverse pressure $\sigma^{st}_{\text{lat},y}$ contributed by any dependable stirrups is calculated from the second term of (1). In redesigning substandard r.c. members for shear resistance, (9) needs to be used both in assessing the residual $V_{n\text{-res}}$ prior to the FRP jacketing intervention and also in evaluating the post-upgrading resistance. Therefore:

$$\begin{aligned} &V_{n\text{-res}}(q_{\text{old}}) = \lambda(q_{\text{old}})\,(V_s + V_c)\\ &V_n(q_{\text{new}}) = \min\{\lambda(q_{\text{old}}), \lambda(q_{\text{new}})\}\,(V_s + V_c) + V^f_w;\\ &V^f_w = \sigma^f_{\text{lat},y} A_g \end{aligned} \tag{10}$$

where q is the behavior factor (or R in FEMA 273 [14]) and $\sigma^f_{\text{lat},y}$ is the transverse pressure in concrete owing to the jacket in the direction of lateral sway (first term of (1)). The shear strength of the jacketed member is the sum of the jacket contribution, V^f_w, and the contribution of the existing mechanisms, namely concrete, V_c, and transverse steel, V_s.

In deriving (10), it has been assumed that the target μ_Δ used in the redesign of the member is equal to the behavior index, q_{new} (or R_{new}), thus, $\mu_\Delta \leq$ 3.5–4 that is currently recommended for new designs (FEMA 273 [14], EC-8 [15]). It is recognized in (10) that the existing mechanisms may have sustained damage during previous loading. For this reason residual rather than the full contributions of core concrete and web reinforcement are considered, by taking the minimum value of λ for these terms, based on the ductility demand suffered during previous events, or used as a target value for redesign. Based on experiments the softening coefficient λ is not applied on the V^f_w as diagonal cracking is suppressed by the application of the jacket (Tastani and Pantazopoulou [1]).

3.3. Anchorage/lap-splice strength calculations

As a rule, a direct consequence of upgrading member resistance through FRP jacketing is to increase the deformation demand in the lap-splice/anchorage regions. Frequent bond related problems in existing construction include, (a) lap splicing of the main bars immediately above the floor level in the anticipated plastic hinge regions without the necessary transverse reinforcement, (b) use of smooth reinforcement where bond capacity depends on the frictional resistance and the formed end-hooks, and (c) use of short development lengths.

To remedy anchorage problems, FRP jackets are wrapped orthogonal to the anticipated splitting plane. Using the ACI 318-02 [7] frictional model for the bond, the development capacity of a given anchorage length L_b is calculated from: $F = 0.5\pi \cdot D_b \cdot L_b \cdot f_b = \mu \cdot \sigma_{\text{lat}} \cdot D_b \cdot L_b$, where μ is the coefficient of friction at the steel–concrete interface and σ_{lat} the pressure exerted upon the lateral surface of the bar by the cover, transverse stirrups and FRP jacket. The average bond stress $f_{b,d}$ is given by,

$$\begin{aligned} f_{b,d} &= \frac{2\mu}{\pi D_b}\left(\sigma^c_{\text{lat}} + \frac{\sigma^{st}_{\text{lat}} + \sigma^f_{\text{lat}}}{N_b}\right)\\ &= \frac{2\mu}{\pi D_b}\left(\zeta \cdot c \cdot f'_t + \frac{k^{\text{anch}}_{\text{st}} A_{\text{st}} f_{y,\text{st}}}{N_b s} + \frac{2k^{\text{anch}}_f n t_f E_f \varepsilon^{\text{eff}}_f}{N_b}\right) \end{aligned} \tag{11}$$

where N_b is the number of bars (or pairs of spliced bars) laterally restrained by the transverse pressure. Note that σ^f_{lat} and σ^{st}_{lat} are obtained from (1) when considering the likely plane of splitting failure through the lap or anchorage—e.g. the crack path to the nearest unrestrained surface and the pertinent effectiveness coefficients for the anchorage; σ^c_{lat} represents the transverse confining pressure exerted by the concrete cover ($\zeta = 1, 2$ either for fully elastic or fully plastic behavior of the concrete cover). For lap splices the likely cover spalling path, p, which depends on the density of bar placement along the cross sectional perimeter would be used instead of c in (11) (Priestley et al. [5]).

The value of $\varepsilon^{\text{eff}}_f$ used in (11), is the surface strain value associated with attainment of bond strength along the bar. For conventional deformed bars bond strength is attained at a bar slip of 0.1–0.2 mm (Tastani and Pantazopoulou [16]). Recent results (Lura et al. [17]) show that at any point along the bar, slip is about twice the radial displacement of the internal bar boundary imposed by the displacing ribs, thus, the associated radial displacement at the bar surface is $u_{r,o} = 0.05$–0.1 mm. The corresponding hoop strain equals the $u_{r,o}$ divided by the radius of the internal boundary, $\varepsilon^{ho} = u_{r,o}/(D_b/2)$. If the change in radial displacement occurring through the cover thickness owing to contraction of concrete is neglected, then the hoop strain at the outside boundary of the cover, where the FRP jacket is installed is: $\varepsilon^{\text{eff}}_f = u_{r,o}/(c + D_b/2) = 2u_{r,o} \cdot [D_b(1 + 2(c/D_b))]^{-1} = \varepsilon^{ho} \cdot (1 + 2(c/D_b))^{-1}$. For example, for $D_b = 20$ mm and $c = D_b$, $\varepsilon^{ho} = 0.005 - 0.01$, and $\varepsilon^{\text{eff}}_f = 0.0017 - 0.003$, a range of values consistent with the empirical strain lower limit of 0.0015 that has been proposed for calculating the jacket stress for lap splices and anchorages (Priestley et al. [5]). The lateral force in (5) required to develop the anchorage or lap splice capacity in the upgraded element is referred to as $V_{\text{anch}} = [\pi D_b L_b f_{b,d} N_b jd + P(d - 0.h)]/L_s$ where jd is the lever arm between the internal reinforcement force and concrete stress resultant and P is the applied axial force.

Thus, particularly for anchorage and lap splice calculations, (11) should be used with the following values for stirrup and FRP-jacket stresses: $\min\{200\text{ GPa} \cdot 0.1/D_b, f_{y,\text{st}}\}$ and $E_f \cdot (\varepsilon^{\text{eff}}_f$ due to slip of the bar), respectively. If greater values are used in (11) for the strains of stirrups and jacket, this should be accompanied by attendant reductions in the value of the shear

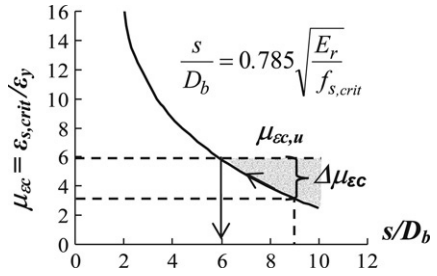

Fig. 6. Relationship between dependable compressive strain ductility, $\mu_{\varepsilon c}$ and s/D_b ratio.

friction coefficient μ so as to reflect the increased level of bond damage.

3.4. Resistance to longitudinal bar buckling in FRP-wrapped r.c. elements

In r.c. members with substandard details, the compression strain capacity of longitudinal reinforcement is often limited by premature buckling owing to the large unsupported length of the bars: stirrup spacing in the range of 200–300 mm is not uncommon in old construction. At this spacing s, the bar slenderness ratio s/D_b is 10–15 for a $D_b = 20$ mm bar, much in excess of the upper limit of 6–8 recommended for high to moderate ductility structures (FIB Bulletin 24 [4]). Due to its susceptibility to local stress concentrations FRP jacketing cannot entirely mitigate rebar buckling (Bousias et al. [18]). If e is the lateral deflection of the buckling rebar from its original alignment, the corresponding local jacket strain is e/R_{ch}, where R_{ch} is the chamfering radius. For $R_{\text{ch}} = 25$ mm, the jacket will reach its ultimate strain ($\approx$0.01) at $e = 0.25$ mm, i.e. while buckling is still imperceptible. Failure is rather brittle, occurring by local rupture of the jacket before it may be mobilized for confinement.

Considering *sideways* buckling (that means, a buckling length equal to stirrup spacing) as would occur in a plastic hinge region with severe shear demand, it may be shown that the critical s/D_b ratio that corresponds to rebar stress $f_{s,\text{crit}}$ is given by $s/D_b = 0.785(E_r/f_{s,\text{crit}})^{1/2}$ where E_r is the double-modulus of steel at the stress level considered (FIB Bulletin 24 [4]). Thus, given the full stress–strain diagram of any given bar, the limiting strain–ductility $\mu_{\varepsilon c} = \varepsilon_{s,crit}/\varepsilon_y$ may be plotted against the s/D_b ratio. Parameter $\varepsilon_{s,\text{crit}}$ is the strain at which the bar will become unstable for the given s/D_b ratio. The example in Fig. 6 refers to steel with $f_y = 400$ MPa, initial strain hardening slope of 30 GPa and a yield plateau to a strain of 0.005.

Theoretically, buckling of any individual bar segment is controlled by its strain–ductility curve, unless the dependable deformation capacity of encased concrete, $\varepsilon_{cc,u}$ ((8a) or (8b)) exceeds the $\varepsilon_{s,\text{crit}}$ value corresponding to the available s/D_b ratio. In that case redistribution between the compressed bars at incipient buckling and the encased concrete is possible, thereby postponing buckling to occur at a higher strain level. Therefore, by increasing the strain capacity of concrete through jacketing to levels higher than $\varepsilon_{s,\text{crit}}$, the effective s/D_b ratio is reduced, as depicted in Fig. 6. The dependable strain ductility of compression reinforcement is:

$$\mu_{\varepsilon c} = \max\left\{\frac{\varepsilon_{s,\text{crit}}}{\varepsilon_y}, \frac{\varepsilon_{s,cu}}{\varepsilon_y}\right\}. \tag{12}$$

An important consideration in detailing the FRP jacket is to ensure that the target displacement ductility of the member after upgrading may be attained prior to buckling of primary reinforcement. To achieve this objective the following steps are required in the design process:

(i) Estimate the target displacement ductility demand at the design performance limit state, $\mu_{\Delta,\text{req}} = \Delta_u^{\text{target}}/\Delta_y$.

(ii) Estimate the curvature ductility demand $\mu_{\phi,\text{req}}$ (where $\mu_\phi = \phi_u/\phi_y$) in the plastic hinge region of the member, using the relationship between μ_Δ and μ_ϕ derived from first principles:

$$\mu_{\Delta,\text{req}} = 1 + 3\left(\mu_{\phi,\text{req}} - 1\right)\frac{l_p}{L_s}\left(1 - 0.5\frac{l_p}{L_s}\right);$$
$$l_p = 0.08L_s + 0.022 f_y D_b. \tag{13}$$

In (13) l_p is evaluated considering yield penetration (Priestley et al. [5]). This expression may require revision for FRP-jacketed members where the contribution of pullout is significant.

(iii) From $\mu_{\phi,\text{req}}$ the compression strain ductility demand, $\mu_{\varepsilon c,\text{req}}$, of compression reinforcement may be estimated. For symmetric displacement reversals during the seismic excitation, it may be shown that $\mu_{\varepsilon c,\text{req}} = 1.1\mu_{\phi,\text{req}} - 1$ (FIB Bulletin 24 [4]).

(iv) Given the available jacket confinement, determine from (12) the available compression strain ductility, $\mu_{\varepsilon c,\text{avail}}$, of primary reinforcement and check if $\mu_{\varepsilon c,\text{avail}} > \mu_{\varepsilon c,\text{req}}$.

If stirrup spacing is such that this requirement may not be satisfied, then an alternative upgrading scheme would be to *opt for increased storey stiffness so as to effect a reduction in the displacement ductility demand* $\mu_{\Delta,\text{req}}$. The lateral force in (5) corresponding to the development of buckling strain in the compression reinforcement is $V_{\text{buckl}} = M_{\text{buckl}}/L_s$. M_{buckl} is obtained from equilibrium of moments in the critical section at attainment of strain $\varepsilon_{s,\text{crit}}$ in the compression reinforcement.

4. Deformation capacity assessment for FRP encased members

To better understand the cyclic load behavior of r.c. prismatic members with substandard detailing (i.e., reinforced with sparse stirrups, smooth primary reinforcement anchored with hooks, inadequate anchorages and/or lap splices in plastic hinge regions) after jacketing with FRPs, a database of tests published in international literature was assembled and analyzed, aiming to assess the relationship between strength and deformation enhancement and the design characteristics of the FRP jackets.

The database table contains over 70 specimens and is given by Tastani and Pantazopoulou [1]. For each specimen the experimental load–displacement envelope is used to define yield and ultimate displacement and lateral load strength, as

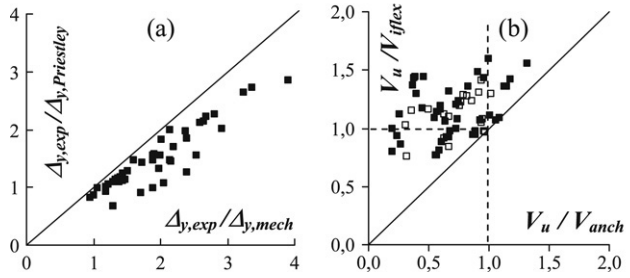

Fig. 7. (a) Comparison between experimental and analytical yield displacement estimates and (b) experimental strength values normalized to the ideal flexural and anchorage strengths (empty square = control, black square = retrofitted specimens).

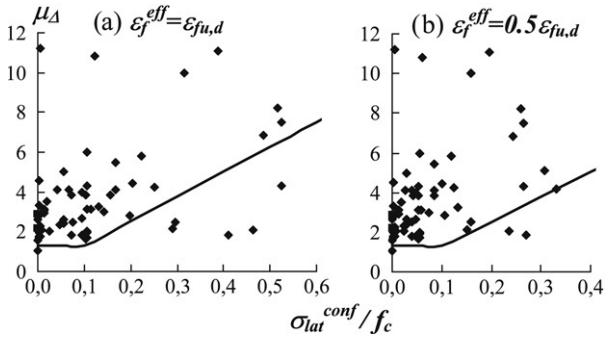

Fig. 8. Correlation of (14) with the experimental data points.

illustrated in Fig. 1: the characteristic points in the envelope correspond to 80% of the peak load, V_u. Fig. 7(a) plots experimental estimates of yield displacement (defined as per Fig. 1) after being normalized by the calculated result from two popular models, i.e.:

1. The estimated yield displacement using classical mechanics ($\Delta_{y,\text{mech}} = \phi_y L_s^2/3$) and
2. the flexural-slip component of the yield-displacement as proposed by Priestley et al. [5] ($\Delta_{y,\text{Priestley}} = \phi_y(L_s + 0.022 f_y D_b)^2/3$, MPa, mm), where ϕ_y is the yield curvature. The shear component is neglected in this calculation because it is deemed insignificant as compared with rotations owing to flexure and reinforcement pullout.

From Fig. 7(a) it is concluded that both analytical estimates fall well below the experimental value for yield displacement with the worse estimates resulting from the classical model. Underestimation of yield displacement indicates that the actual slip contribution is larger than calculated.

For all specimens, the ideal flexural strength V_{iflex} was calculated from first principles considering the material properties given by the researchers. The FRP confinement or strain-hardening of the embedded reinforcement were not considered, thereby representing the flexural resistance of the member prior to upgrading (the confining action of embedded stirrups has been accounted for). From evaluation of the test results it is confirmed that the behavior under cyclic loading is improved through FRP jacketing to the extent that premature brittle failure modes are suppressed (shear, lap splice failure) so that ductility owing to yielding of embedded flexural steel may be realized. In most cases, failure was marked by excessive slippage of longitudinal reinforcement from the support (Fig. 7(a)). Few cases report crushing of the concrete compression zone accompanied by buckling of longitudinal reinforcement.

Fig. 7(b) plots the observed strength V_u of the upgraded member normalized by the calculated value of V_{iflex} on the y-axis, and by the calculated value of V_{anch} on the x-axis. V_{anch} was calculated as per Section 3.3 detailed in the preceding, using the following values for the parameters: $f_t' = 0.5 f_c'^{0.5}$, $k_{\text{st}}^{\text{anch}} = 0.33$, $\zeta = 1$, $\mu = 1.4$ and $u_{r,o} = 0.05$ mm. In the case of bars anchored in a footing stub the contribution of the FRP was neglected; for spliced bars in the plastic hinge region the FRP contribution was taken into account where in the cover contribution the critical crack path p was used instead of c in (11). In Fig. 7(b) all datapoints are clustered left to the equal value line showing that in any case the anchorage or splice strength was greater than the ideal flexural strength. Datapoints below the horizontal dashed line refer to specimens that failed prematurely by shear ($V_u < V_{\text{iflex}} < V_{\text{anch}}$). Datapoints lying above and left of the dashed lines denote a limited ductile response up to failure ($V_{\text{iflex}} < V_u < V_{\text{anch}}$). The rest of the data right of the vertical dashed line denote a very ductile response with exhaustion of all anchorage reserves ($V_{\text{iflex}} < V_{\text{anch}} < V_u$). Note that the control specimens in Fig. 7(b) are represented by empty squares whereas the retrofitted by filled squares.

Most of the experimental points are clustered above the equal value line (Fig. 7(b)) underscoring the localization of deformation demand that occurs in the anchorage, which, after jacketing, becomes the weak link of the upgraded member as regards response in terms of deformation. Further study would be required to assess those cases where flexural failure was marked by excessive slip because under the simultaneous presence of axial load the P–Δ effects would decimate the dependable flexural strength—this parameter is only marginally affected by the FRP jacket, and hence this problem may need to be *controlled* through global stiffening of the structure.

Through FRP jacketing all failure modes but flexural yielding of reinforcement are suppressed. This is manifested by the ductility in the load–displacement curve of the upgraded member. In this study, the database was correlated with an empirical *lower bound* expression for the available displacement ductility, μ_Δ as a function of transverse confining pressure $\sigma_{\text{lat}}^{\text{ave}}$ calculated from (2):

$$\mu_\Delta = 1.3 + 12.4 \times \left(\frac{0.5\left(k_f^c \rho_{fv} E_f \varepsilon_f^{\text{eff}} + k_{\text{st}}^c \rho_{sv} f_{y,\text{st}}\right)}{f_c'} - 0.1 \right) \geqslant 1.3. \tag{14}$$

Fig. 8 compares the experimental values with the analytical estimates of (14); these were obtained using either $\varepsilon_f^{\text{eff}} = \varepsilon_{fu,d}$ (Fig. 8(a)) or $\varepsilon_f^{\text{eff}} = 0.5\varepsilon_{fu,d}$ (Fig. 8(b)) so as to evaluate the conservatism implicit in (14). Experimental points lying below the proposed design curve correspond to repair cases where

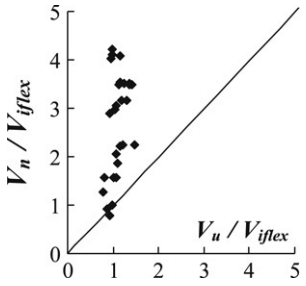

Fig. 9. Correlation of database with (10) for estimating shear strength of FRP jacketed elements.

the postrepair yield displacement used to quantify dependable ductility from the load displacement envelope was the apparent value, markedly greater than the true displacement at first steel yielding. Clearly the second option (Fig. 8(b)) is overly conservative (assuming $\varepsilon_f^{\text{eff}} = 0.5\varepsilon_{fu,d}$ the datapoints are moved to the left) and is not considered further when (14) is used in detailing.

Shear strength of the repaired/strengthened elements calculated from (10) is plotted in Fig. 9 against the experimental values, V_u. All values have been normalized with the ideal flexural strength, V_{iflex}. Evidently flexural failure prevailed in all cases after jacketing, whereas (10) is deemed conservative.

5. Global considerations when using FRP jackets for seismic upgrades

Most of the strength terms in the critical design equation (5) depend on the anticipated deformation demand in the member after the repair. Once the strength of the weakest strength mechanism is exhausted, localization of deformation is expected to occur in that particular mode of behavior, which becomes the fuse of the member response upon increased deformation demand. The collective evaluation of the database presented above demonstrated that FRP jacketing of deficient r.c. members increases their nominal deformation capacity, but it affects adversely the anchorage. A large component of the drift levels attained in jacketed column tests is owing to lumped rotation resulting from pullout of primary reinforcement from the anchorage within a single crack.

Although FRPs cannot entirely mitigate bar buckling they effectively increase the dependable strain capacity of compression reinforcement by enhancing the toughness of the encased concrete core through confinement. However, stiffness of FRP jacketed members remains unaffected; to this end it is useful to employ pertinent criteria in order to identify whether the upgrading measures need to involve storey stiffening along with local interventions through FRP jacketing. The response indices that may be used as diagnostic tools in assessing the global adequacy of the structural morphology at least for the pre-yield stage are, (i) empirical upper bound estimations of the fundamental period T, as: $T < 0.1N_s$ for r.c. frames, and $0.05N_s < T < 0.075N_s$ for r.c. frame-walls, where N_s is the number of storeys, (ii) the magnitude of drift at yield of the vertical elements (0.5% is a reasonable upper bound for frame structures, 0.25% for walls), (iii) the fundamental translational mode-shape of the structure that may reveal the existence of soft storeys. For linear elastic behavior the fundamental mode shape may be a sufficient test, because any discontinuities in stiffness or mass will be captured by relative normalized drift ratios that significantly exceed the mean value of $1/N_s$.

In designing the upgrading scheme, the seismic demand need be determined in displacement terms (ATC-40 [19]). Prerequisite is idealization of the structure as an equivalent single degree of freedom system (ESDOF) through a selected empirical approximation of the predominant shape of lateral vibration and calculation of the corresponding stiffness (secant to yield). The estimated period and vibration shape can be used with any of the criteria (i)–(iii), in defining the upgrading strategy.

For immediate results the ESDOF properties may be used with the YPS (Yield Point Spectra) of the design earthquake in order to evaluate the anticipated displacement demand and corresponding displacement ductility (Aschheim and Black [20]). The primary advantage of YPS over the capacity spectrum (EC-8 [15]) is that it may be used to guide design decisions without iteration or even calculation of the complete pushover envelope. The slope of the radial line to any point of the elastic spectrum is ω^2/g (ω is the frequency, g is the acceleration of gravity). The ratio of the system's normalized yield force V_y^{ESDOF} (point A on the radial line), to the elastic spectral ordinate V_e^{ESDOF} is the required system ductility (using the equal displacement rule, Fig. 10(a)). The corresponding elastic spectral displacement is the target displacement of the inelastic system: $\Delta_u = S_d$. For a preliminary assessment of the suitability of the upgrading scheme it is acceptable to adopt an upper limit of 2% for the lateral drift of the structure at the design earthquake. For larger displacement levels second order effects that are usually not efficiently mitigated by concrete encasement need be explicitly addressed in the upgrading strategy. The critical displacement limit, $\Delta_{u,\text{crit}} = 2\%H$ (where H is the building height) corresponds to a spectral limit of $\Delta_{\text{crit}}^{\text{ESDOF}}$. The vertical line in the ADRS drawn at displacement $\Delta_{\text{crit}}^{\text{ESDOF}}$ defines a design boundary. Acceptable solutions are to the left of the vertical line and above the YPS associated with the limiting ductility of the system. By also implementing stiffening schemes in the structure, the radial line is effectively rotated counterclockwise in the ADRS, thereby reducing the design value of Δ_u, with an attendant mild increase in the required V_y^{ESDOF}. Note that a larger increase in capacity may be required to also reduce the target μ value.

The final step in the design is to apply the analytical expressions for each of the ultimate limit states discussed as per the qualitative equation (5), thereby linking the target indices of behavior with the jacket dimensions.

In lieu of more detailed conclusions, this section demonstrates implementation of the proposed design framework in an example case study. The objective is to explore the extent to which FRP jacketing could mitigate the vulnerability of flexible substandard structures and to illustrate through this example the advantages and the limitations of the method.

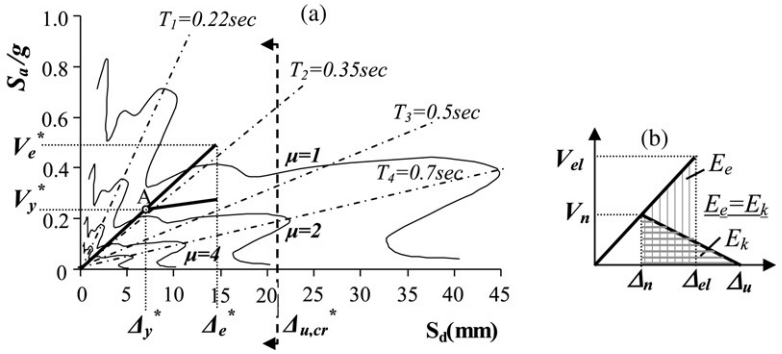

Fig. 10. Isoductile YPS for ATH3 long—(a) definition of values (the superscript * denotes the abbreviation ESDOF) and (b) equivalence of kinetic energies: to dissipate the attracted kinetic energy the structure displaces inelastically to collapse.

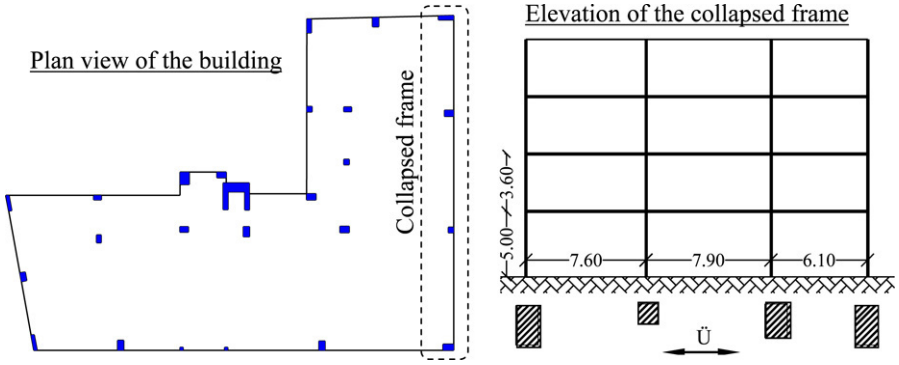

Fig. 11. Plan view of the building and elevation plan of the collapsed frame.

Table 1
Basic properties of pilotis columns

Col. ID	kl_u/r	$P/A_g f'_c$	K_i (kN/m)	$V_{i,\text{flex}}$ (kN)	Δ_y (mm)	V_n^{ideal} (kN)	Δ_n (mm)	V_N^{failure} (kN)	$V_{n,\text{req}}$ (kN) = $K_i \times \Delta_v^{\text{ave}}$	$M_{P-\Delta}/M_y$
C_1	32	0.09	2880	103.4	35.97	77.6	27	75.0	103.4	0.09
C_2	36	0.42	1162.5	74.73	63.87	80.3	>63.87	30.5	43.9	0.43
C_3	32	0.19	2370	96.97	40.71	91.8	38.55	62.1	89.4	0.19
C_4	32	0.07	2880	103.4	35.97	72.4	25.17	75.0	103.4	0.07
Total	–	–	**9300**	**378.5**	Δ_y^{ave}**= 37.6 mm**	**322.1**	Δ_n^{ave}**= 26.1 mm**	**242.6**	**340**	–

6. Example: Application in a four-storey frame with pilotis

The frame considered resembles a component of a four-storey structure with pilotis that collapsed during the 1999 Athens Earthquake (Fig. 11). It had three similar spans of 7.6 m, 7.9 m and 6.1 m respectively. Column dimensions are taken as $C_1 = 0.40 \times 0.70$ m, $C_2 = 0.35 \times 0.35$ m, $C_3 = 0.40 \times 0.60$ m and $C_4 = 0.40 \times 0.70$ m in the pilotis and are reduced to 0.35×0.60 m, 0.35×0.35 m, 0.35×0.50 m and 0.35×0.60 m in the upper floors. Due to their orientation in the floor plan, the columns bent about their weak axis during lateral sway of the frame. The first floor height is taken as 5 m; upper floors had a 3.6 m typical height. Nominal material strengths correspond to the $C25$ and $S400$ classifications of EC-2 [21]. Transverse reinforcement was rather sparse and is simulated herein by rectangular stirrups $\Phi 6/300$ mm ($S220$). Tension and compression reinforcement ratios are taken as 0.90% each for columns C_1 and C_4, and 0.75% for columns C_2 and 0.50% for C_3.

A preliminary evaluation of column slenderness points to a dramatic lack of stiffness: all columns had a ratio (kl_u/r, Table 1) over 30, exceeding the upper limit of 22 for sway frames as per ACI 318-02 [7] (stability index Q – or θ as per the EC-8 [15] – equals $P_{\text{tot}}\Delta_y^{\text{ave}}/(V_y l) = 0.08 > 0.05$, where P_{tot} is the total axial load, $\Delta_y^{\text{ave}} = 36.7$ mm, $V_y = 340$ kN refers to the yielding of the stiffer columns and $l = 5000$ mm is the effective height of the first floor columns, Table 1). The relevant properties of all first storey columns are listed in Table 1 (column stiffnesses, K_i, defined at flexural yielding, displacement at yielding, Δ_y, column nominal shear

Table 2
Calculation of required jacket layers for each design action (n to be rounded off to next integer)

Col. #	Confinement for $\mu_{\Delta,\text{req}} = 2.5\, l_p \approx 350$ mm (Priestley [5])				Bar buckling (strain capacity of conf. core: $\varepsilon_{cc,u} = 0.011$, Eq. (8b))			Shear increase		Lap-splice above base (Eq. (11))
	$\sigma_{\text{lat}}^{\text{ave}}/f_c'$	k_f^c	ρ_{fv}% (Eq. (14))	n	$\mu_{\varepsilon c,\text{avail}}$ (Eq. (12))	$\mu_{\phi,\text{req}}$ (Eq. (13))	$\mu_{\varepsilon c,\text{req}} = 1.1\,\mu_{\phi,\text{req}} - 1$	V_w^f (kN)	n	avail. $L_b = 20D_b$ for all columns:
C_1	0.2	0.37	0.8	7.5 $\varepsilon_{cc,u}/\varepsilon_y = 5.6$		4.6	4.1 < 5.6	49.1	0.3	$f_{bd}^{\text{avail}} = 2.5$ MPa
C_2		0.54	0.5	3.6		5.1	4.7 < 5.6	<0	—	$f_{bd}^{\text{req}} = 5.0$ MPa
C_3		0.43	0.7	6.1		4.9	4.4 < 5.6	25.2	0.2	$\sigma_{\text{lat}}^f/N_b = 54$ (N/mm)
C_4		0.37	0.8	7.5		4.6	4.1 < 5.6	52.8	0.3	$n = 3.6$ ($\varepsilon_f^{\text{eff}} = 0.13\%$)

strength $V_n = V_c + V_s$ (where $\beta = 0.3$); V_s supported by the sparse column web reinforcement is only 46.4 kN, whereas for the calculation of V_c the gravity axial load has been considered). Also listed is the ideal flexural capacity at column yielding, V_{iflex}. The lateral stiffness of the first storey, K_{pilotis}, is obtained from column contributions. Accounting for the masonry infills in the upper floors, stiffness and mass vectors, the corresponding mode fundamental mode shape and associated period are estimated:

$$\underline{K} = K_{\text{pilotis}}\,\{1, 89, 89, 89\}; \quad K_{\text{pilotis}} = 9300\ \text{kN/m}$$
$$\underline{M} = m_o\,\{1, 0.92, 0.92, 0.84\}; \quad m_o = 98.4\ \text{kN s}^2/\text{m}$$
$$T = 1.24\ \text{s}; \qquad \underline{\Phi} = \{0.984, 0.992, 0.997, 1\}.$$

The remarkably long fundamental period underlines the lack of stiffness in this structure (based on the criteria listed in the preceding the fundamental period ought to be less than 0.4 s). From the ATH3 long ADRS spectrum (5% damping) the elastic spectral ordinates are, $S_a = 0.088$ g and $S_d^{el} = S_a/\omega^2 = 34$ mm, which after transformation results in a building displacement $\Delta_{el} = 34.34$ mm. The resulting elastic base shear is $V_{el} = K_{\text{pilotis}} \cdot \Delta_{el} \cdot \Phi_{1,1} = 314.4$ kN, much higher than the available base shear strength. Shear failure would be anticipated at a lateral force of $V_n = 242.6$ kN and displacement of $\Delta_n = 26.1$ mm, well before flexural yielding at 378.5 kN (or at 340 kN when assuming yielding of the stiffer elements). To dissipate the kinetic energy of the system, the structure would displace inelastically (on the softening branch, Fig. 10(b)) by an amount: $\Delta_u = 26.1\ \text{mm} + (314.4 + 242.6) \times (34.34 - 26.1)/242.6 = 45$ mm. This magnitude of collapse displacement is consistent with reconnaissance observations and results from DRAIN-3D simulations of the structure.

Upgrading with FRP jackets only would maintain the soft-storey function of the pilotis. In such an option, the column shear strength would need be increased so as to exceed the force required to yield the stiffer columns (C_1, C_3, C_4). The average horizontal yield displacement would be $\Delta_y^{\text{ave}} = \text{ave}\{36, 36, 40.7\} = 37.6$ mm, corresponding to a storey drift of 0.75%, while the C_2 remains elastic at an estimated force of 43.9 kN $= k_2 \times 37.55$ mm, Table 1). The total design lateral force for dimensioning the column jackets would be 340 kN with $\mu = 314.4/340 = 0.9$.

Columns C_2 and C_3 combine a high slenderness ratio with a moderately high axial load. At the target design drift of 0.75% the second order moments exceed 10% of the respective column yield moments (Table 1). A proper upgrading scheme would be either to reduce slenderness possibly by r.c. jacketing of those columns, or by addition of a shear wall for stiffness. Considering the high magnitude of second order effects it is desirable that the unaltered system may support a dependable deformation capacity up to 2% lateral drift (a ductility of $\mu_\Delta = 2.5$), with a simultaneous shear strength increase to the ideal flexural yielding force (=340 kN). FRP jackets are detailed for the columns using the procedures described in the present work. Results are listed in Table 2 for each design action (shear, anchorage, rebar buckling) with the associated number of required layers identified separately. Material properties used in the calculations include CFRP wraps with $t_f = 0.13$ mm, $f_{fu} = 3500$ MPa, $\varepsilon_{fu,d} = 0.015$, and $E_f = 230$ GPa. Jackets are taken as fully wrapped (closed), thus, the effective strain used in the calculations is $\varepsilon_f^{\text{eff}} = 50\%\,\varepsilon_{fu,d}$ for shear and rebar buckling. In Table 2, each mode of failure considered leads to a different number of required layers. The more severe requirement in terms of jacket thickness is associated with the anchorage, oversupplying the demands of the other response mechanisms. It is worth noting that whereas actual failure occurred by shear, theoretically a single jacket layer would suffice to upgrade column shear strength to levels exceeding the ideal flexural strength.

Acknowledgment

The work presented in this paper was funded by the Greek Organization for Seismic Protection (OASP) through the project ENIKAS.

References

[1] Tastani S, Pantazopoulou SJ. Strength and deformation capacity of Brittle R.C. members jacketed with FRP Wraps. In: CD-ROM proceedings of the fib-symposium on concrete structures in seismic regions. Athens (Greece): Technical Chamber of Greece (Ed.); 2003.
[2] ACI Committee 440. Guide for the design and construction of externally bonded FRP systems for strengthening concrete structures (ACI 440.2R-02). Farmington Hills (Michigan): American Concrete Institute; 2002.
[3] Pantazopoulou S. Role of expansion on mechanical behavior of concrete. ASCE J Struct Eng 1995;121(12):1795–805.

[4] FIB Bulletin 24. Seismic assessment and retrofit or R.C. buildings. Report by task group 7.1. Lausanne (Switzerland): International Federation for Concrete; 2003 [Chapter 4].
[5] Priestley M, Seible F, Calvi M. Seismic design and retrofit of bridges. New York: J. Wiley and Sons Inc.; 1996.
[6] FIB Bulletin 14. externally bonded FRP reinforcement for R.C. structures. Report by task group 9.3. Lausanne (Switzerland): International Federation for Concrete; 2001.
[7] ACI Committee 318. Building code requirements for structural concrete and commentary (ACI 318-02). Farmington Hills (Michigan): American Concrete Institute; 2002. 1323 pages.
[8] Brēna S, Wood S, Kreger M. Full-scale tests of bridge components strengthened using carbon FRP composites. ACI Struct J 2003;100(6): 775–84.
[9] Chaallal O, Shahawy M, Hassan M. Performance of axially loaded short rectangular columns strengthened with carbon FRP wrapping. ASCE J Compos Constr 2003;7(3):200–8.
[10] Richart F, Brandtzaeg A, Brown R. A study of the failure of concrete under combined compressive stresses. Engrg. Experiment Station Bull. #185 1928.
[11] Tastani SP, Pantazopoulou SJ, Zdoumba D, Plakantaras V, Akritidis E. Limitations of FRP jacketing in confining old-type reinforced concrete members in axial compression. ASCE J Compos Constr 2006;10(1): 13–25.
[12] Moehle J, Elwood K, Sezen H. Gravity load collapse of building frames during earthquakes. In: S.M. Uzumeri symposium behavior and design of concrete structures for seismic performance. ACI-SP 197; 2002.
[13] EKOS-2000. Greek code for reinforced concrete. Technical Chamber of Greece; 2000. www.oasp.gr.
[14] NEHRP guidelines for the seismic rehabilitation of buildings. Washington DC: Federal Emergency Management Agency; 1997.
[15] Eurocode 8. Design provisions for earthquake resistance of structures (EC-8). Brussels: European committee for standardization; 1998.
[16] Tastani SP, Pantazopoulou SJ. Limit state model for bond of machined steel bars: Experimental results. In: CD ROM proceedings 2nd international fib congress. 2006.
[17] Lura P, Plizzari G, Riva P. 3D finite-element modelling of splitting crack propagation. Mag Concrete Res. 2002;54(6):481–93.
[18] Bousias N, Triantafillou T, Fardis M, Spathis L, O'Regan B. Fiber-reinforced polymer retrofitting of rectangular R.C. columns with or without corrosion. ACI Struct J 2004;101(4):512–20.
[19] ATC-40. Seismic evaluation and retrofit of concrete buildings. Report no. SSC96-01. California: Applied Technology Council and Seismic Safety Commission; 1996.
[20] Aschheim M, Black E. Yield point spectra for seismic design and rehabilitation. EERI Earthq Spectra 2000;16(2):317–36.
[21] Eurocode 2. Design of concrete structures (EC-2). Brussels: European Committee for Standardization; 2002.